Electron line densities and meteor masses calculated from models and meteor radar measurements

G. Stober, Ch. Jacobi

Zusammenfassung

Die Methoden zur Beobachtung des atmosphärischen Windfeldes und der Temperatur im Mesopausenbereich mit Meteorradaren sind gut bekannt. Im Gegensatz dazu gibt es nur wenige Informationen über die Eigenschaften der Meteore (Größe, Dichte und Masse), die durch ein Meteorradar detektiert werden können. Im Folgenden sollen die physikalischen Prozesse, die beim Eintritt eines Meteoroiden in die Atmosphäre von Bedeutung sind, genauer betrachtet werden. In Baggaley (2002) und Stober et al. (2007) wurde eine theoretische Beschreibung des vom Radar empfangenen Signals gegeben. Die Modelle, die in Hunt et al. (2003) vorgestellt wurden, wurden im Hinblick auf die besondere Geometrie des am Collm (51.3°N,13°E) befindlichen Meteorradars untersucht und mit Messungen des Systems in Bezug gesetzt. Damit überhaupt ein Vergleich durchgeführt werden kann ist es notwendig das Radar zu kalibrieren, d.h. die an den Antennen empfangenen Signale müssen in eine vom Meteorschweif reflektierte Leistung umgewandelt werden. Dazu werden die Ergebnisse, die in Campistron (2001) vorgestellt wurden, auf das SKiYMET Radar am Collm angewendet. Aus den kalibrierten Daten und unter Verwendung einer empirischen Klimatologie ist es möglich die Masse der Meteore abzuschätzen.

Abstract

The methods to observe the atmospheric wind field and the temperature in the mesopause region using meteor radars are well known. In contrast, there are only a some information about the properties of the meteors (size, density and mass), which can be detected by a meteor radar. In the following the physical processes, which are of importance for a meteoroid entering the earth's atmosphere, are considered. In Baggaley (2001) and Stober et al. (2007) a theoretical description of the signal received by the radar was given. The models evaluated in Hunt et al. (2003), will be discussed considering the specular geometry of the Collm meteor radar (51.3°N,13°E) and compared to the measurements. This comparison is only possible with a calibrated radar, which means that the received arbitrary amplitudes are converted into the reflected power from the meteor trail. Therefore, the results shown in Campistron et al. (2001) will be applied for the Collm SKiYMET radar. With the calibrated data and the assignment of an empirical climatology it is possible to give an estimate of the meteor mass.

1   Introduction

When meteoroids enter the earth's atmosphere they form a cylindrical plasma trail, which mainly expands due to ambipolar diffusion. The creation of the plasma is described by the conventional meteor ablation theory developed by McKinley (1961) and Ceplecha et al. (1998). In principle the impinging air molecules decelerate the meteoroid and ionize the atoms at the

surface. Assuming conservation of momentum and energy allows a mathematical treatment of this problem.

The aim of this study is to get some knowledge about the size and mass of the meteors detected by the meteor radars. A direct measurement is not possible, but using atmospheric models like MSIS00 or CIRA86 and making some assumptions about the density and shape of the meteors allows to calculate these parameters. Therefore we investigated these models under this point of view. It is well-known that there are three species of meteors with different densities ranging from 1000 kg/m^3 to 7800 kg/m^3. But the species with the highest probability (90%) are stony meteoroids with a density of approximately 3400 kg/m^3. For all results presented in this study, the shape is assumed to be spherical.

One of the key points investigating the meteor mass is the electron line density, which is a directly measured parameter by the radar, in the case of a calibrated system itself. McKinley (1961) gave a mathematical description of the signal power returned from a specular echo meteor trail. However, the meteor radars just measure a voltage at the antenna, which has to be converted into a power, considering all the losses due to the cables and the system. For a radar operating in the VHF band most of the noise enters the system as cosmic background radiation. This noise has a strong diurnal oscillation and can be used as a reference to calibrate the radar. This technique is straightforward and can be performed during normal operation.

The paper is organized as follows: in section 2 a description of the models is given, the numerical results of this models are presented in section 3, the fourth section deals with the measurement of electron line densities and the final section shows a comparison of the results.

2 Meteor ablation models

Three different models are presented in this study, which are based on single body ablation theory. Therefore, the conservation of momentum and energy is of importance for all three models. Parameters that will be used are given in Tab. 1. Hunt et al. (2003) compared the so called two equation and three equation models, which are based on the theoretical work by Öpik (1958). A descending meteor encounters per time interval a defined air mass dm equal to $A_{cross}\rho_{air}vdt$, which forces a meteoroid to decelerate. This relation is easy to understand under the assumption of momentum conservation. The first model uses a simple Monte Carlo (MC) simulation to calculate the deceleration of the meteoroid, which means that the mass of the impinging air molecules is given by their atomic mass. A pseudo random number generator selects the position where an atmospheric atom will hit the meteor and the geometry at this position defines the momentum that is transferred to the meteor body. However, the computational time does not allow to simulate an acceptable time span dt. This problem is solved by a scaling factor. There is only one assumption necessary for this procedure, namely that dt has to be chosen small enough, so that no severe changes in air density and mass loss of the meteor occur. The advantage of this model is, that it is not necessary to know the drag coefficient for the calculation of the deceleration. This is important especially for randomly structured or fractal meteor surfaces. But such objects will not be considered in this study.

The two equation model consists of two differential equations based on the theoretical studies done by Öpik (1958) which describe the deceleration and mass loss of the meteor;

$$\frac{dv}{dt} = -\frac{1}{m} A_{cross} \, c_d \, \rho_{air} \, v^2 \quad , \tag{1}$$

$$\frac{dm}{dt} = -A_{cross} \, c_d \, \rho_{air} \, \sigma_a \, v^3 \quad . \tag{2}$$

symbol	quantity/source	value/source
dv/dt	deceleration	-
dm/dt	mass loss due to ablation	-
dT/dt	temperature gradient	-
T	temperature	-
T_0	atmospheric temperature	$150-750K$
A	surface area	-
A_{cross}	cross section area	-
β	ionization efficiency	-
Λ_s	sputtering efficiency	-
σ_{SB}	Stefan-Boltzmann constant	$5.67\cdot10^{-8}W/m^2K^{-4}$
σ_a	ablation parameter	$10^{-8}s^2/m^2$
C_1	constants in Hunt et al. 2003	$6.92\cdot10^{11}kg/m^2s^{-1}K^{1/2}$
C_2	constants in Hunt et al. 2003	$57800...80000K$
C_3	constants in Hunt et al. 2003	$1\cdot10^3J/kgK^{-1}$
Q	constants in Hunt et al. 2003	$7\cdot10^3J/s$
C	heat capacity	$0.8...0.95kJ/kgK^{-1}$
m	meteor mass	$10^{-6}...10^{-14}kg$
m_a	mass of the ablated meteor species	$4.98\cdot10^{-26}kg$
v	meteor velocity	-
v_{thres}	threshold velocity	$5-8km/s$
c_d	drag coefficient	$0.2..1.17$
M_r	radio magnitude	-
ρ_{air}	air density	taken from MSIS00
ρ_{met}	meteor density	$1000...8000kg/m^3$
ε	emission	$0.5...0.95$

Table 1: Physical symbols and basic values used in the models.

The mass loss equation is the same for the two equation model and the MC simulation. There is only one empirical parameter, the ablation coefficient σ_a, which defines the amount of mass that can ablate. The value used here was taken from Hunt et al. (2003) and Verniani (1973). During the calculations σ_a was kept constant. Measurements with radio telescopes indicated a variation of the ablation parameter in the range of $10^{-6.4}-10^{-8.5}\ s^2/m^2$. A value of $10^{-8}\ s^2/m^2$ corresponds to a meteor mass of $10^{-9}kg$. Hunt et al. (2003) investigated only the two equations (1) and (2) for their calculations of the electron densities. But, the temperature as a very important parameter is missing in the first model equations. This is solved by assuming energy conservation and using the heat transfer coefficient Λ, which allows a calculation of the quantity dT/dt;

$$\frac{dT}{dt} = \frac{A_{cross}\,c_d\,\rho_{air}\,v^3}{Q\,m} - \frac{\varepsilon\,A\,\sigma_{SB}\,(T^4-T_0^4)}{Q\,m}\ .\tag{3}$$

The third model is more sophisticated. It allows the treatment of processes like sputtering and evaporation. The greatest benefit of this model is, that the mass ablation is no longer described by a constant independent of the temperature. Baggaley (2002) stated the need of a minimum temperature, which is necessary to start the ablation process on the meteor surface. This behavior is also supported in the study of Hill et al. (2005), who investigated high altitude meteors. Hill et al. (2005) found a threshold energy for the impinging molecules to start the process of sputtering. In the three equation model these effects are included by a temperature dependent sputtering efficiency;

$$\Lambda_s = Q\,(6\cdot10^{-16})e^{\frac{T}{290}}\ .\tag{4}$$

For this model the temperature-time dependency becomes more complicated; there are three terms which describe the friction, the radiation losses and the ablation heat;

$$\frac{dT}{dt} = \frac{A_{cross}\, \rho_{air}\, v^3}{2\, C_3\, m}(1 - \Lambda_s) \;-\; \frac{\varepsilon\, A\, \sigma_{SB}\, (T^4 - T_0^4)}{C_3\, m} \;-\; \frac{A_{cross}\, C_1\, Q}{m\, C_3\, T^{\frac{1}{2}}} e^{\frac{-C_2}{T}} \;. \tag{5}$$

For high temperatures the ablation heat term dominates, which causes a rapid meteor mass loss. This is counterbalanced by a much smaller mass loss during flight times with lower temperatures. This leads directly to the mass loss equation, which consists of the two processes, the mass loss due to sputtering and the normal friction induced mass loss;

$$\frac{dm}{dt} = -\frac{A_{cross}\, c_d\, C_1}{T^{\frac{1}{2}}} e^{-\frac{C_2}{T}} \;-\; \frac{\Lambda_s\, \rho_{air}\, A_{cross}\, v^3}{2\, Q} \;. \tag{6}$$

From equation (6), it is obvious that two regimes for a meteor are important. If the meteor does not reach a sufficiently high temperature (approximately $T < 1800\, K$) the mass loss is small and the meteor will decelerate without significant ablation. The second case is for extremely high temperatures (approximately $T > 2700\, K$), which leads to in an incredible high ablation rate and the meteor completely vanishes. For this case the radiation term cannot counter balance the rate of heating. Among this temperatures the meteor shows similar characteristics compared to the other models.

Solving the equations enables to calculate the electron line density assuming Jones (1997) ionization efficiency;

$$\beta = 9.4 \cdot 10^{-6} (v - v_{thres})^2 \cdot v^{0.8} \;. \tag{7}$$

There the threshold velocity defines the velocity at which a certain atom can no longer be ionized by the impinging molecules. This velocity is the lowest limit to produce significant ionization. Hence, as soon as a meteor reaches the threshold velocity the computation stops. Using the Jones (1997) ionization efficiency permits to calculate the electron line density for the meteor flight path according to;

$$q = \frac{\beta}{m_a\, v}\frac{dm}{dt} \;. \tag{8}$$

The electron line density depends only on the velocity and the forces acting on a meteoroid. Using the MSIS00 climatology the last unknown parameter is given by the aerodynamic active surface. Assuming a spherical geometry and a mean density taken from astrophysical studies (Unsöld/Baschek, 2005) about meteors allows a direct relation to the meteor mass.

Finally, we introduce the radio luminosity, which is a helpful parameter to understand the limits of radio visibility (micro meteor limit 12^{mag}). In analogy to visible astrophysical observations we define this radio luminosity (Baggaley, 2002) as:

$$M_{rmag} = 36.8 \;-\; 2.5 log(q) \;+\; 2.5 log(v/1000) \;. \tag{9}$$

3   Single Body Ablation Theory - Numerical Results

Finally, for the numerical calculations we need some assumptions about the meteor parameters like geometry, density, initial mass and velocity, as well as the angle of atmosphere entrance

(AOAE). Computational time and the known parameters with the respective to the radar give the boundaries for the simulations. Most of the meteors are detected by the radar in the height range from 75-105 km altitude with the highest event rate close to 90 km. The velocity distribution shows a spread from 6 km/s to 40 km/s. There also exists some information about the AOAE corresponding to the angle given by elevation angle from the radar, which defines the maximal entry angle. Considering all this external factors makes 150 km a good starting altitude for the simulation and for the minimum height, as lower boundary, 70 km is selected. The air density and temperature are taken from the MSIS00 model. The starting temperature of the meteor is also given by the model at the starting height, because the meteor body should be in equilibrium with the environmental atmosphere at this altitude.

Assuming spherical geometry ($c_d = 0.5$) and constant meteor density during one run allows the numerical computation of all important meteor time dependencies. In the simulations we also set the heat transfer coefficient $\Lambda = 1$. This means that all available energy is transferred as heat to the meteor.

By solving the differential equations with a 4th order Runge-Kutta algorithm a complete time dependent behavior for all three models is derived in each run. The time step was set variable to ensure numerical stability. In the cases investigated here a constant time step $dt = 1/2144 s$ was used. This equals to the PRF (Pulse Repetition Frequency) of the meteor radar at Collm observatory.

The velocity plot (fig. 1) shows the very smooth deceleration of the meteor above 120 km. Obviously there is a critical height before the air gets dense enough to exert a force on the meteor. This height depends on the mass and the velocity. In the first 30 km of its flight path the meteor slows down by less than 5% of the initial velocity and does not have a significant mass loss fig. 2.

The deceleration plot reveals much more details about the forces acting on the meteor. Obviously, at around 90 km altitude the strongest force is exerted to the meteor (fig. 1). This is exactly the same altitude where the maximum flux of meteor trails occurs. All three models show almost the same altitude of the maximal force, while only the absolute values differ. This is explained by the mass loss equation (6), which depends on the temperature for the three equation model. This dependency allows the meteor to ablate much stronger at lower altitudes, because of the fact that there is a threshold temperature before the meteor can start to ablate significantly. This temperature is approximately 1800 K (fig. 2), which is also mentioned by Baggaley (2002).

In the temperature vs. altitude plots (fig. 2) the models show qualitatively the same behavior, which becomes more clear by the fact that the heat transfer coefficient is constant $\Lambda = 1$ for the MC simulation and the 2 equation model, but it depends on the temperature for the 3 equation model and varies among 0.6 and 1 (fig. 2). The mass loss is the most critical parameter for the models, because from this the electron line density is defined. Fig. 2 shows the differences among the models, the MC and 2 equation model let almost ablate the meteor up to 95% of its initital mass, while the three equation model does not predict that this amount is ablated. The reason is the short time of ablation. The meteor decelerates at such a high rate that a significant ablation cannot start and the meteor is slowed down before it can reach the temperature to get the sputtering process dominant. This means that the radiative cooling is able to balance the heating process, before it becomes strong enough to start significant sputtering.

Fig. 3 shows the relation of the electron line density produced by the meteor and the radio magnitude. A meteor radar has a limit of detection which depends on the frequency (Singer et al., 2004). This limit is approximately $10^{-12} \, m^{-1}$. Hence, a meteor with an initial mass of $10^{-9} \, kg$ is at the lower limit to produce this electron line density. But as fig. 2 shows, the mass at the specular point can be below this limit due to the ablation. The blue line in fig. 3 gives the micro
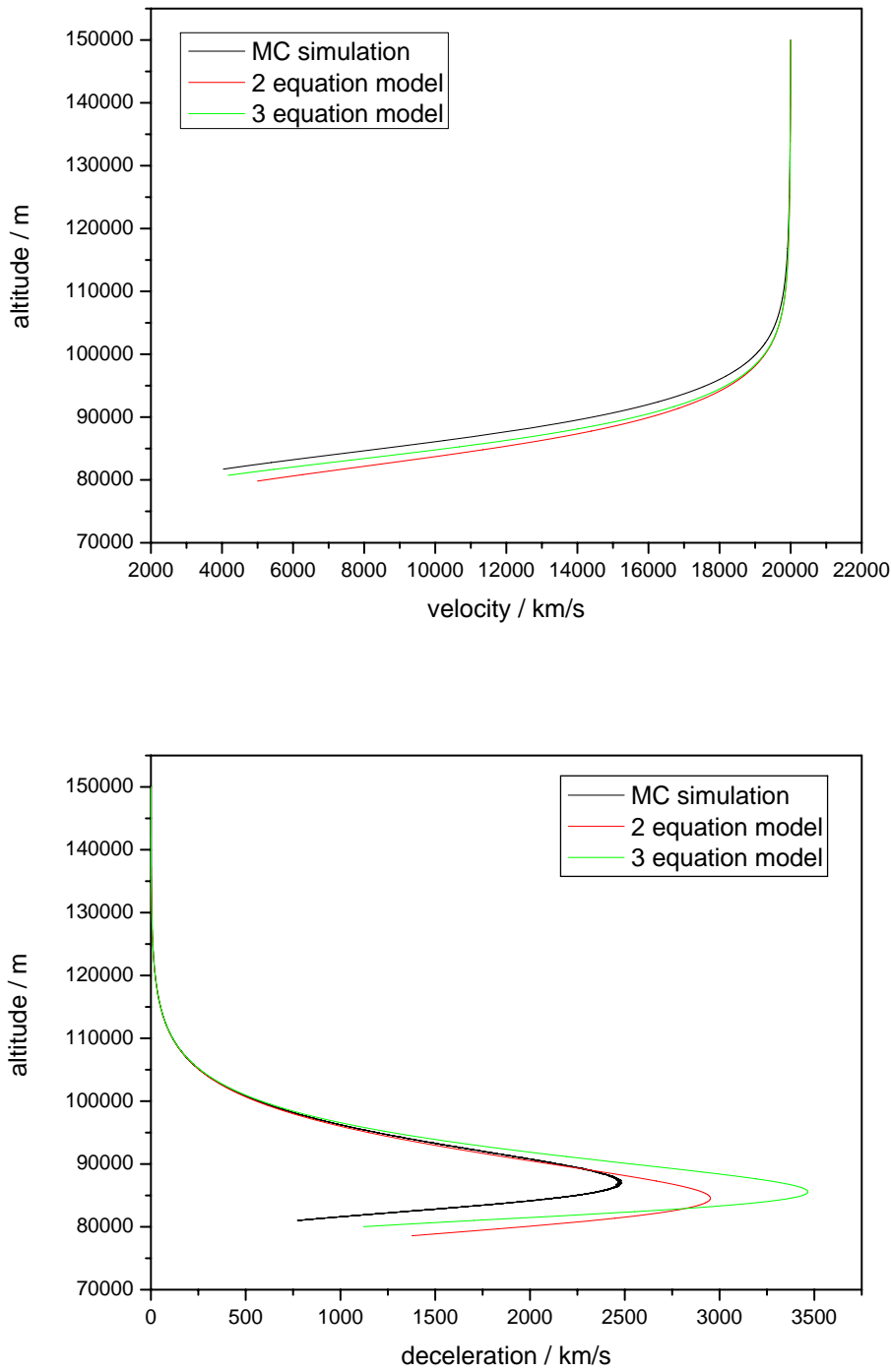
Figure 1: Velocity and deceleration profiles for a meteor of 10^{-9} kg and a density of 3400 kg/m^3.

meteor limit which has a magnitude of approximately $r_{mag} = 12$. Below this limit a detection is impossible and the meteor would remain invisible for the system. All models deliver higher values for meteors of mass 10^{-9} kg in the altitude range between 100 km and 85 km.
The shown results are only partly independent of other meteoric parameters. The altitude where the maximal force is exerted on a meteor is independent from the velocity, but the absolute value
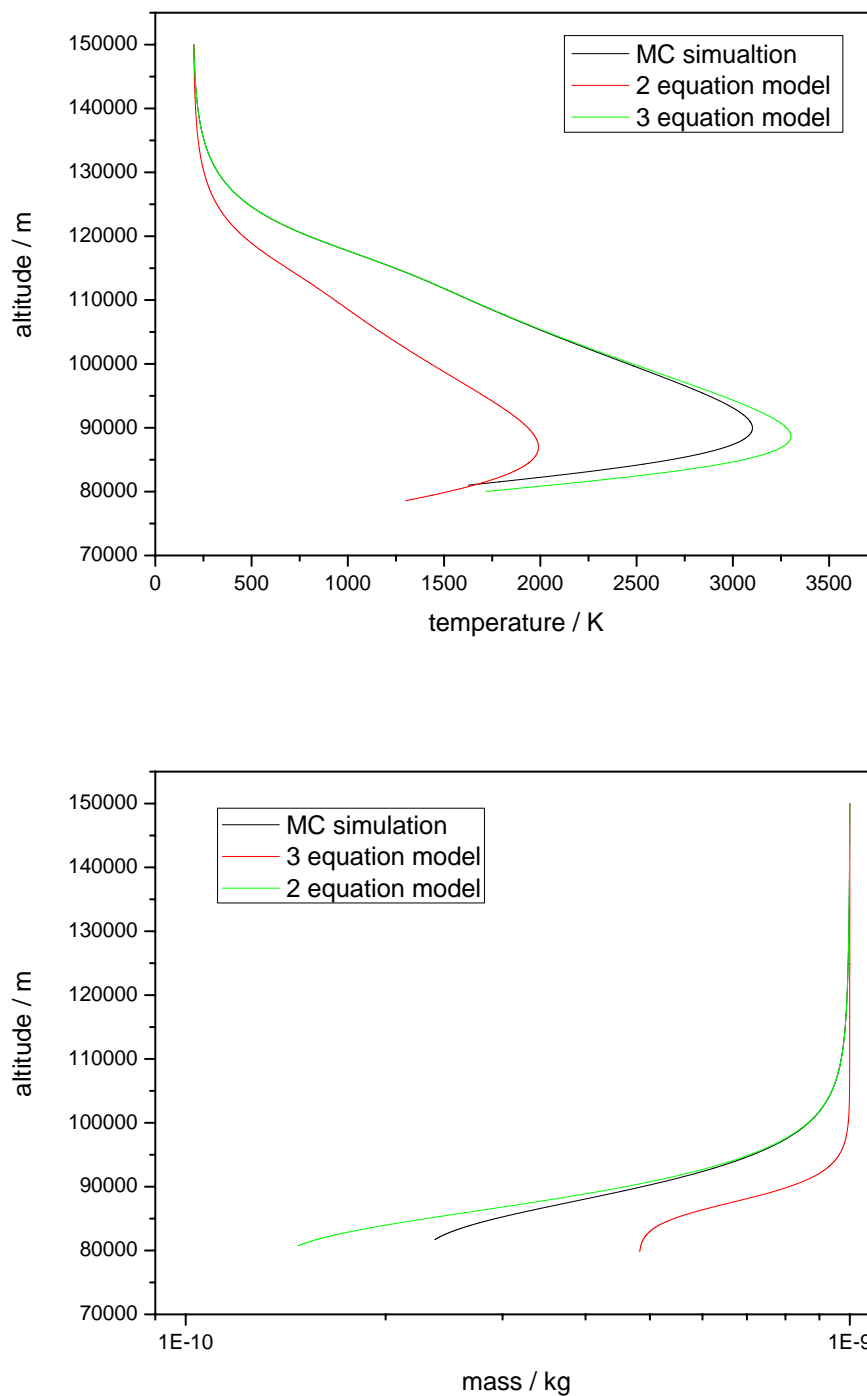
Figure 2: Temperature and mass profiles for a meteor of 10^{-9} kg and a density of 3400 kg/m^3.

scales with it. This is also the case for the temperature profiles, which remain qualitatively the same, but the maximum temperature depends on the velocity. For the 3 equation model this leads to the effect that a very fast meteor $v > 50$ km/s completely ablates and for slow speeds $v = 11$ km/s, which is the minimal atmospheric entry speed, the meteor does not even start to ablate.
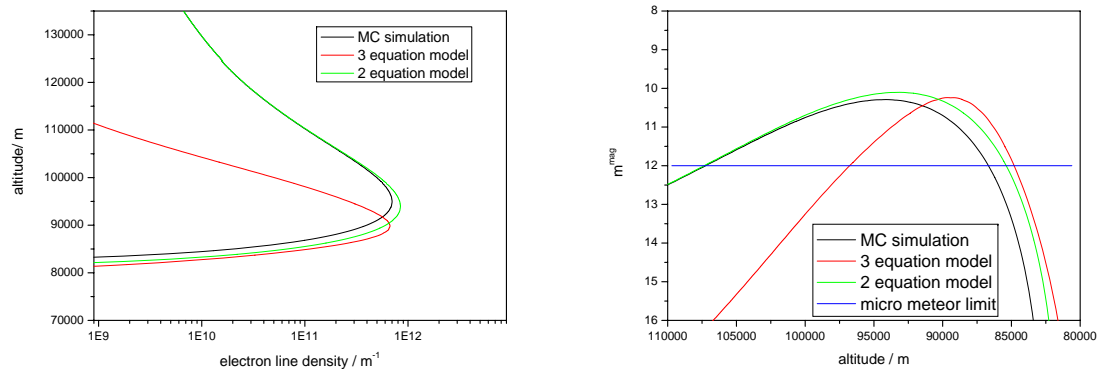
Figure 3: Electron line density and radio magnitude profiles for a meteor of $10^{-9}\ kg$ and a density of $3400\ kg/m^3$.

The AOAE also has only an influence on the absolute values. A shallow entry leads to a slow deceleration, which means that the ablation is small. This results in a reduced maximum electron line density, but the signal persists longer. In contrast a steep entry leads to a in very quick deceleration and a rapid increase of the meteor temperature, which can cause a complete ablation for high velocities, because the radiation term cannot compensate the strong heating.

The density is also an important parameter, so it is obvious that less dense meteors are decelerated in higher altitudes than denser objects. This can explain the occurrence of high altitude meteors, which were reported by Fujiwara et al. (1998). Thus, iron meteoroids can penetrate deeper into the atmosphere than stony meteors of the same weight.

Furthermore we also calculated the meteor entry for different masses ranging from $10^{-6} - 10^{-12}\ kg$ and found that the heavier meteors start to decelerate at lower atmospheric regions. So a stony meteor with a mass of $10^{-7}\ kg$ will not start to ablate significantly until passing an altitude of 90 km. A meteor close to the micro meteor limit will exert the maximum force at approximately 100 km altitude.

4   Calibration of the meteor radar using sky temperature maps

Campistron et al. (2001) investigated the possibility to use VHF ST (Stratosphere - Troposphere) radars to measure astronomical issues during routine meteorological surveys. Their study is based on five VHF ST radars operating at 45 MHz and 52 MHz, at latitudes from 43.133°N-48.628°N and longitudes from 0.367°E-8.717°E. These systems have five beams (1 vertical and 4 oblique) with beam widths of 5.6° and 6.5°. For the measurement a dwell time of 15 min was used to ensure proper accuracy (+/-600K).

Due to the fact that cosmic radiation is variable it is necessary to get a reference sky radiation map. Typically this map is expressed as a sky temperature. The source of the radiation are interactions of ray electrons and the galactic magnetic field (Alvarez et al., 1996). Hence, the sky temperature depends on the frequency of observation. Within the VHF band we have:

$$\frac{T_1}{T_2} = \left(\frac{f_1}{f_2}\right)^{-\beta_s} . \tag{10}$$

In the literature the spectral index β_s is assumed constant within a limited frequency range. There were several observations from 22 MHz to 408 MHz (Roger et al. 1999), which found that β_s is variable in the range of 2.4 - 2.55 (Milogradov-Turin and Smith, 1973). For Collm

meteor radar operating at 36.2 MHz we use $\beta_s = 2.5$.

In fig. 4 the measured noise amplitudes from the Collm radar are compared to the reference sky temperature taken from Campistron et al. (2001) given in galactic coordinates (declination δ, Right Ascension α) for $\delta = 59°$. In the northern hemisphere there are two major noise sources, Cassiopeia A ($\alpha = 19h59.49'$, $\delta = 40°44.26'$) and Cygnus A ($\alpha = 23h23.44'$, $\delta = 58°49.47'$). The VHF ST radars can resolve these sources as peaks in the temperature map. The meteor radar has an all sky coverage and so these sources will appear much more smoothed compared to the VHF ST radars. Therefore, the data for all angles larger than $\alpha = 20h$ was removed to avoid this problem. Obviously the noise amplitude at Collm fits very good the diurnal oscillation of the sky temperature map derived by Campistron et al. (2001) (fig. 4). This enables us to fit the data with a linear model fig. 4 (right) to convert the noise amplitude to a sky temperature. The next step in the process of calibration is to estimate the noise power from this sky temperature. Singer et al. (2004) used the simple expression;

$$P_{noise} = (T_{sky} + T_r)k_b B \ . \tag{11}$$

$B = 50kHz$ is the bandwidth of the receiver, k_B the Boltzmann constant, T_{sky} the sky temperature and T_r the receiver noise temperature. Considering that only echoes above the 10 db noise floor can be detected (Singer et al. 2004) allows to calculate the noise power or directly the reflected power of the meteor echoes. This leads, according to McKinley (1961), to the electron line density for the meteor;

$$q^2 = \frac{P_R R^3}{2.5 \cdot 10^{-32} P_T G_R G_T \lambda^3} \ , \tag{12}$$

where P_R is the reflected radar power, P_T the transmitted power, G_R and G_T are the antenna gains, R the specular distance and λ the wavelength of the radar. For the Collm radar the antenna gains were calculated after McKinley (1961). The so derived electron line densities are accurate within 10%, assuming that the error is mainly due to the linear fit ($R^2 = 0.96$) and the inaccuracies of the reference sky temperatures.

This procedure delivers reasonable results for measurements calibrated with a delay bridge as done by Singer et al. (2008). This method feeds defined fractions of the transmitted pulse, which were delayed by $100\mu s$, directly in the antenna receivers instead of a signal. Singer et al. (2008) investigated the difference of weak/strong meteors in the decay time and found a correspondence in the electron line densities for these meteors. So the electron line density for weak/strong meteors maximises for $8.0^{11} - 2.0^{12}/2.0^{12} - 7.0^{12}$ m^{-1}. The calibration for the Collm radar delivers similar quantities for the electron line densities, which illustrates that a sky temperature map is a possibility to calibrate such a system.

5   Results

The height distribution measured by the meteor radar (fig. 5) and the simulated deceleration curve for a stony meteoroid with a mass of 10^{-9} kg show similar characteristics (fig. 3). There is also a very good coincidence among the model and radar derived electron line densities. Therefore we used the MSIS00 climatology and calculated the meteor masses from measured electron line densities (fig. 7), assuming a spherical geometry and a meteor density of 3400 kg/m^3. It is also possible to use an empirical mass-radio luminosity relation to derive the masses of the meteors (Verniani, 1973). This relation is less accurate, because it can only provide a minimum mass for a velocity range (fig. 8). This dependency allows calculating a minimum detectable
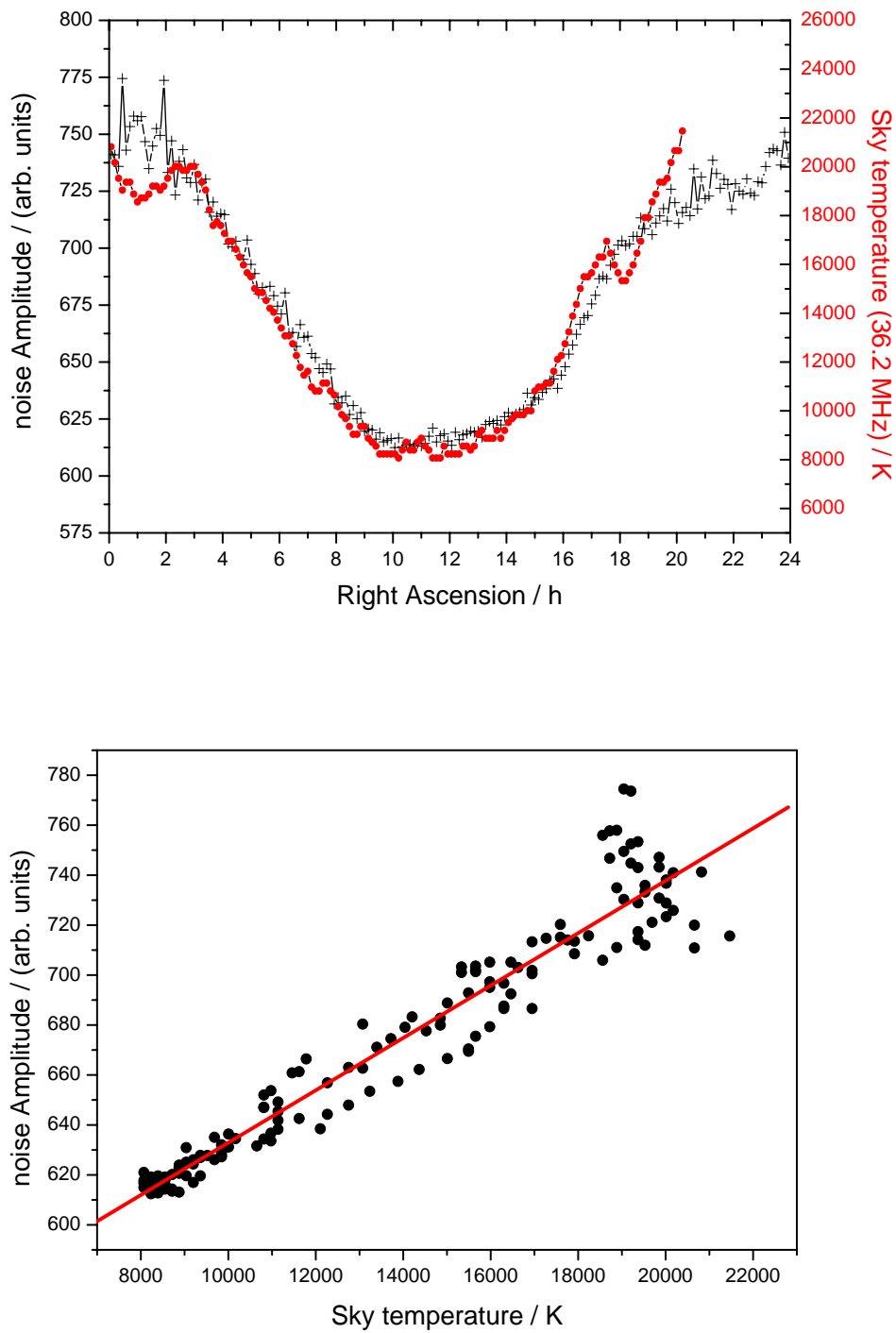
Figure 4: Plots of Sky temperature from Campistron et al.(2001) $\delta = 59°$ (red) and the noise amplitude from the Collm meteor radar (black).

mass for a certain velocity bin, considering the detection threshold for the radar. The threshold can be estimated (Singer et al., 2004) again using a sky temperature as major noise source. A meteor must be one order of magnitude brighter to be detected.

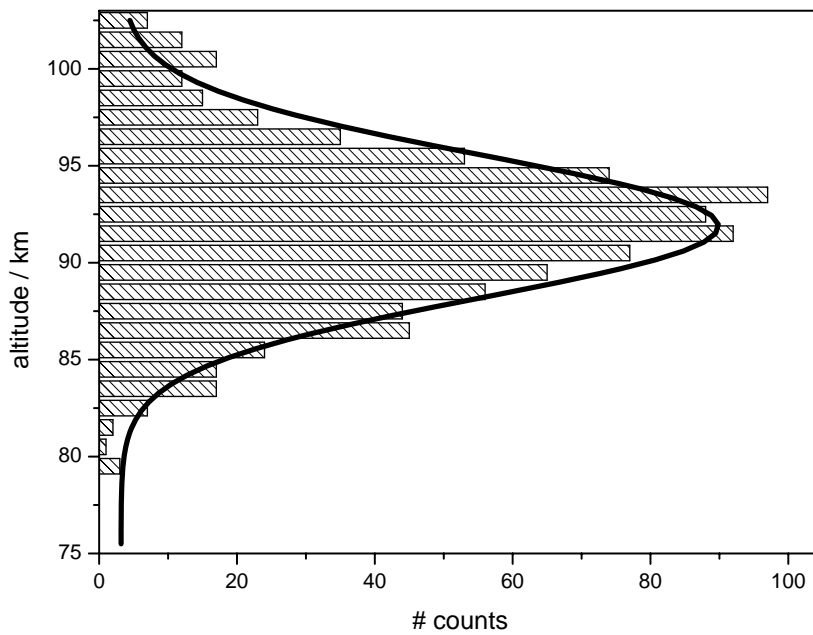Both histograms show a peak at masses of 10^{-10} kg (fig. 7 and 8), which is about one order of

Figure 5: Histogram of the height distribution for all meteors, were it was possible to estimate the specular velocity.
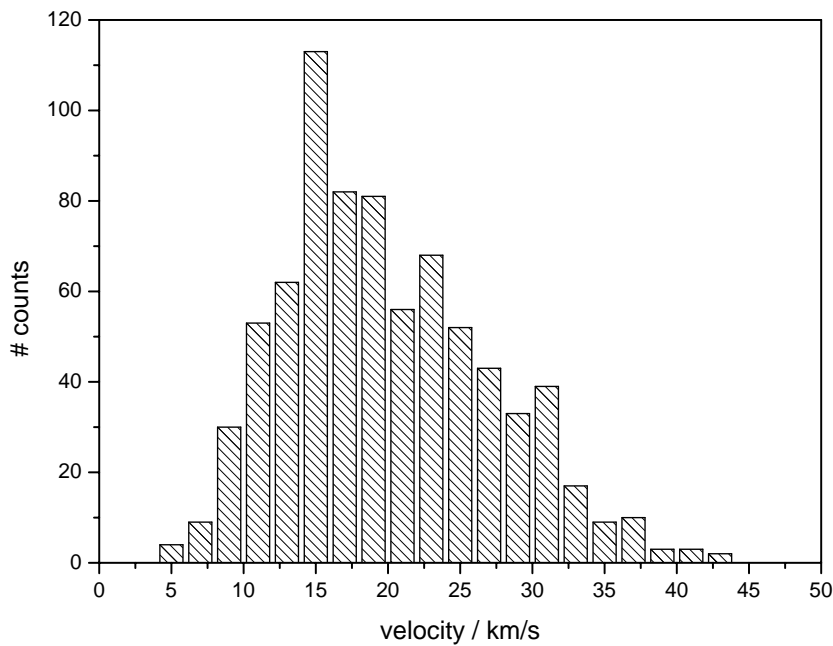

Figure 6: A typical velocity distribution measured at Collm with a meteor radar.

magnitude smaller than the initial mass for the simulation, and can be explained by the fact that we measure most of the meteors at an altitude of 90 *km*. The meteors ablated already 50-60% of their mass at the specular point (fig. 3). The same effect happens by analysing our measured
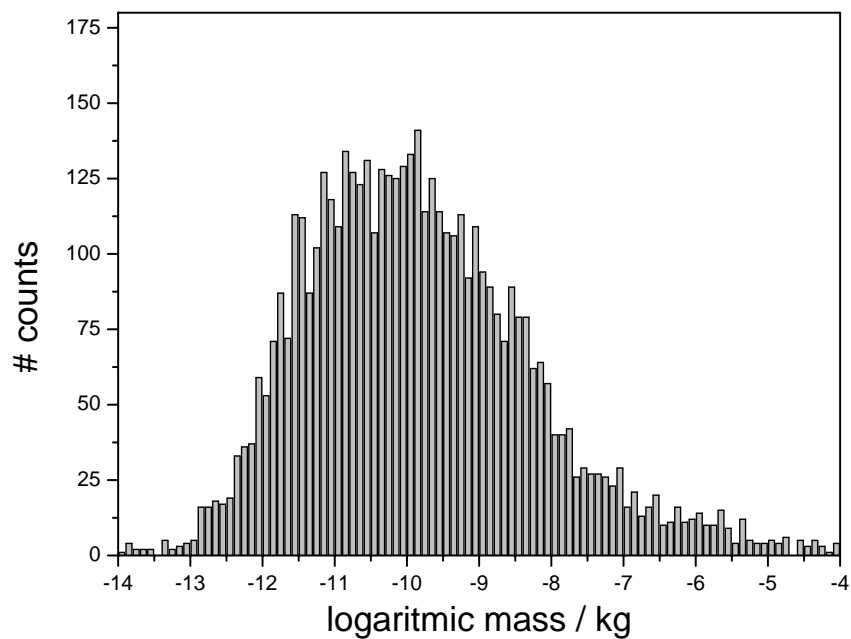
Figure 7: Histogram of meteor masses measured with the meteor radar Collm.
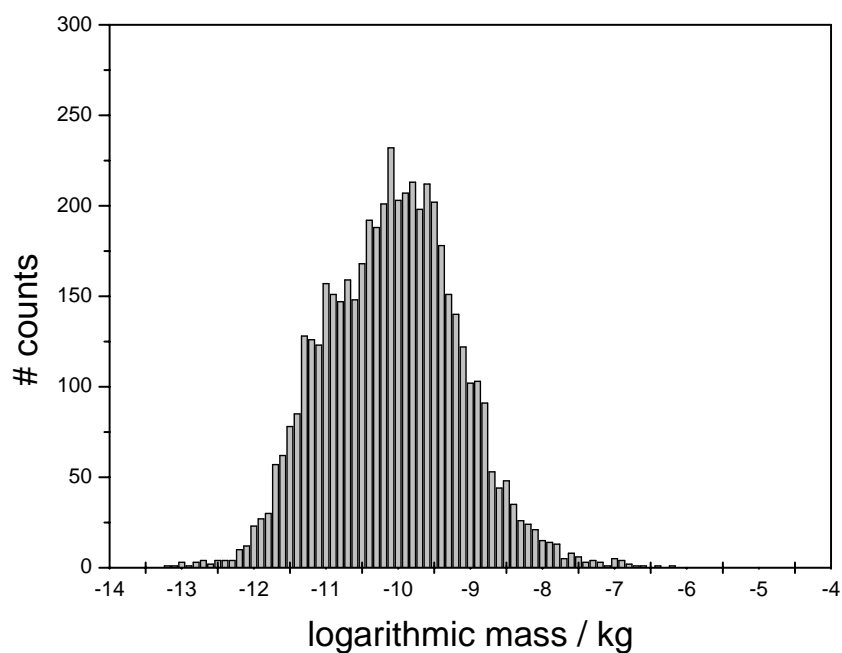

Figure 8: Histogram of estimated masses using the semi-empirical mass - radio luminosity relation derived by Verniani (1973).

velocity histogram (fig. 6). There is a peak at velocities around $15 - 25$ km/s, which means that the initial velocity of the meteors can be much higher depending on their altitude. A meteor

detected at 85 *km* altitude lost almost 50-70% of its initial speed (fig. 3). But this loss rate depends on all the parameters we used in the calculation, which makes it difficult to give a reliable estimate of the initial velocity for a meteor with such a measurement.

The differences in the histograms concerning the span of meteor masses are explainable by the fact that the semi empirical method from Verniani (1973) can provide only a minimum mass for a meteor at a velocity, which leads together with our average meteor density to reduced meteor masses for the heavier meteors. Considering all the uncertainties from the model and the meteor parameters, the total error is about one order of magnitude. The mean error between both methods of mass estimation is by a factor of two, with a standard deviation of 0.7 orders of magnitude.

6   Conclusion

The comparison between models and measurement indicates that stony meteors with masses from $10^{-8} - 10^{-9.5}$ *kg* are the most probable species to be detected by a standard meteor radar. But the good coincidence of the height distribution and the maximum deceleration force is no evidence for that. There are too many empirical parameters and assumptions in the models, that can cause problems within the analysis. However, this study demonstrates that it is possible in principle to determine meteoroid masses with a standard meteor radar, without any changes in the experimental setup. To improve the data quality of the system and to increase the accuracy of the measurements it is necessary to improve the velocity measurement of the radar and to get a better understanding of the chemical properties of the meteors (density and shape). Singer et al. (2008) showed that the temperature measurements can be improved by separating weak and strong meteors. This was achieved by calibrating the radar with a delay bridge between transmitter and receiver and opened the chance for this study. In the future, the investigation of meteor showers with known chemical properties (Geminids, Perseids and Quadrantids) will provide much more precise measurements of the meteor mass for the shower meteoroids.

References

Alvarez H., J. Aparici, J. May, and F. Olmos, A 45 MHz continuum survey of the southern hemisphere, Astron. Astrophys. Suppl. 124, 315-328, 1997

Baggaley W.J., 2003: Radar Observations. in: I.P. Williams, E. Murad (Eds.), Meteors in the earth atmosphere, Cambridge University Press, 123-148, 2002

Campistron B., G. Despaux, M. Lothon, V. Klaus, Y. Pointin, and M. Mauprivez, A partial 45 MHz sky temperature map obtained from the observations of five ST radars, Annales Geophysicae 19, 863-871, 2001

Ceplecha Z., J. Borovicka, W.G. Elford, D.O. Revelle, R.L. Hawkes, V. Porubcan, and M. Simek, Meteor phenomena and bodies, Space Sci. Rev. 84, 327-471, 1998

Fujiwara V., M. Ueda and Y. Shiba, Meteor luminosity at 160 km altitude from TV observations for bright Leonid meteors, Geophys. Res. Lett. 25, 285288, 1998

Hunt S.M., M. Oppenheim, S. Close, P.G. Brown, F. McKeen, and M. Minardi, Determination of the meteoroid velocity distribution at the Earth using high-gain radar, Icarus 168, 12, 34-42, 2003

Jones W.,: Theoretical and observational determinations of the ionization coefficient of meteors, Monthly Notices to The Royal Astronomical Society, 288, 9951003, 1997.

McKinley D.W.R., Meteor Science and Engineering, McGraw-Hill, Toronto, 1961

Milogradov-Turin J., and F. G. Smith, A survey of the radio background at 38 MHz, Mon. Not. R. astr. Soc. 161, 269-279, 1973.

Roger R. S., C. H. Costain, T. L. Landecker, and C. M. Swerdlyk, The radio emission from the galaxy at 22 MHz, Astron. Astrophys. Suppl. 137, 7-19,1999.

Öpik E.J., Physics of Meteor Flight in the Atmosphere, Interscience (New York), 1958

Unsöld A., B. Baschek, DER NEUE KOSMOS Einführung in die Astronomie und Astrophysik 7. Auflage, Springer-Verlag Berlin Heidelberg New York, 90-97, 2005.

Singer W., R. Latteck, L.F. Millan, N.J. Mitchell, and J. Fiedler, Radar Backscatter from Underdense Meteors and Diffusion Rates, Earth Moon Planets, Doi 10.1007/s110308-007-9220-0, in press

Singer W., U. von Zahn, and J. Weiß, Diurnal and annual variations of meteor rates at the arctic circle, Atmos. Chem. Phys. 4, 1355-1363, 2004

Stober G., Ch. Jacobi, Meteor head velocity determination, Sci. Rep. Met. Inst. Univ. L. 41, 47-56, 2007

Verniani F., An analysis of the physical parameters of 5759 faint radio meteors, J. Geophys. Res. 78, 1973

Addresses of Authors:

Gunter Stober, Christoph Jacobi, Institute for Meteorology, University of Leipzig, Stephanstr. 3, 04103 Leipzig, stober@uni-leipzig.de